

Direct evidence for high-energy particle acceleration in the shell of a supernova remnant

F. A. Aharonian¹, A. G. Akhperjanian², K.-M. Aye³, A. R. Bazer-Bachi⁴, M. Beilicke⁵, W. Benbow¹, D. Berge¹, P. Berghaus^{6,a}, K. Bernlöhr^{1,7}, O. Bolz¹, C. Boisson⁸, C. Borgmeier⁷, F. Breitling⁷, A. M. Brown³, J. Bussons Gordo⁹, P. M. Chadwick³, V. R. Chitnis^{10,20,b}, L.-M. Chounet¹¹, R. Cornils⁵, L. Costamante^{1,20}, B. Degrange¹¹, A. Djannati-Atai⁶, L. O'C. Drury¹², T. Ergin⁷, P. Espigat⁶, F. Feinstein⁹, P. Fleury¹¹, G. Fontaine¹¹, S. Funk¹, Y. A. Gallant⁹, B. Giebels¹¹, S. Gillessen¹, P. Goret¹³, J. Guy¹⁰, C. Hadjichristidis³, M. Hauser¹⁴, G. Heinzelmann⁵, G. Henri¹⁵, G. Hermann¹, J. A. Hinton¹, W. Hofmann¹, M. Holleran¹⁶, D. Horns¹, O. C. de Jager¹⁶, I. Jung^{1,14,c}, B. Khélifi¹, Nu. Komin⁷, A. Konopelko^{1,7}, I. J. Latham³, R. Le Gallou³, M. Lemoine¹¹, A. Lemièrè⁶, N. Leroy¹¹, T. Lohse⁷, A. Marcowith⁴, C. Masterson^{1,20}, T. J. L. McComb³, M. de Naurois¹⁰, S. J. Nolan³, A. Noutsos³, K. J. Orford³, J. L. Osborne³, M. Ouchrif^{10,20}, M. Panter¹, G. Pelletier¹⁵, S. Pita⁶, M. Pohl^{17,d}, G. Pühlhofer^{1,14}, M. Punch⁶, B. C. Raubenheimer¹⁶, M. Raue⁵, J. Raux¹⁰, S. M. Rayner³, I. Redondo^{11,20,e}, A. Reimer¹⁷, O. Reimer¹⁷, J. Ripken⁵, M. Rivoal¹⁰, L. Rob¹⁸, L. Rolland¹⁰, G. Rowell¹, V. Sahakian², L. Saugé¹⁵, S. Schlenker⁷, R. Schlickeiser¹⁷, C. Schuster¹⁷, U. Schwanke⁷, M. Siewert¹⁷, H. Sol⁸, R. Steenkamp¹⁹, C. Stegmann⁷, J.-P. Tavernet¹⁰, C. G. Théoret⁶, M. Tluczykont^{11,20}, D. J. van der Walt¹⁶, G. Vasileiadis⁹, P. Vincent¹⁰, B. Visser¹⁶, H. J. Völk¹, S. J. Wagner¹⁴

1 Max-Planck-Institut für Kernphysik, P.O. Box 103980, D 69029 Heidelberg, Germany

2 Yerevan Physics Institute, 2 Alikhanian Brothers St., 375036 Yerevan, Armenia

3 University of Durham, Department of Physics, South Road, Durham DH1 3LE, U.K.

4 Centre d'Etude Spatiale des Rayonnements, CNRS/UPS, 9 av. du Colonel Roche, BP 4346, F-31029 Toulouse Cedex 4, France

5 Universität Hamburg, Institut für Experimentalphysik, Luruper Chaussee 149, D 22761

Hamburg, Germany

6 Physique Corpusculaire et Cosmologie, IN2P3/CNRS, Collège de France, 11 Place Marcelin

Berthelot, F-75231 Paris Cedex 05, France

7 Institut für Physik, Humboldt-Universität zu Berlin, Newtonstr. 15, D 12489 Berlin, Germany

8 LUTH, UMR 8102 du CNRS, Observatoire de Paris, Section de Meudon, F-92195 Meudon

Cedex, France

9 Groupe d'Astroparticules de Montpellier, IN2P3/CNRS, Université Montpellier II, CC85, Place

Eugène Bataillon, F-34095 Montpellier Cedex 5, France

10 Laboratoire de Physique Nucléaire et de Hautes Energies, IN2P3/CNRS, Universités Paris VI &

VII, 4 Place Jussieu, F-75231 Paris Cedex 05, France

11 Laboratoire Leprince-Ringuet, IN2P3/CNRS, Ecole Polytechnique, F-91128 Palaiseau, France

12 Dublin Institute for Advanced Studies, 5 Merrion Square, Dublin 2, Ireland

13 Service d'Astrophysique, DAPNIA/DSM/CEA, CE Saclay, F-91191 Gif-sur-Yvette, France

14 Landessternwarte, Königstuhl, D 69117 Heidelberg, Germany

15 Laboratoire d'Astrophysique de Grenoble, INSU/CNRS, Université Joseph Fourier, BP 53, F-

38041 Grenoble Cedex 9, France

16 Unit for Space Physics, North-West University, Potchefstroom 2520, South Africa

17 Institut für Theoretische Physik, Lehrstuhl IV: Weltraum und Astrophysik, Ruhr-Universität

Bochum, D 44780 Bochum, Germany

18 Institute of Particle and Nuclear Physics, Charles University, V Holesovickach 2, 180 00 Prague 8, Czech Republic

19 University of Namibia, Private Bag 13301, Windhoek, Namibia

20 European Associated Laboratory for Gamma-Ray Astronomy, jointly supported by CNRS and MPG

- (a) now at Université Libre de Bruxelles, Faculté des Sciences, Campus de la Plaine, CP230, Boulevard du Triomphe, 1050 Bruxelles, Belgium
 - (b) now at Tata Institute of Fundamental Research, Homi Bhabha Road, Mumbai 400 005, India
 - (c) now at Washington Univ., Department of Physics, 1 Brookings Dr., CB 1105, St. Louis, MO 63130, USA
 - (d) now at Department of Physics and Astronomy, Iowa State University, Ames, Iowa 50011-3160, USA
 - (e) now at Department of Physics and Astronomy, Univ. of Sheffield, The Hicks Building, Hounsfield Road, Sheffield S3 7RH, U.K.
-

A significant fraction of the energy density of the Interstellar Medium of our Galaxy exists in the form of high-energy charged particles (cosmic rays). Despite almost a century of investigation the origin of these particles remains uncertain. While it is generally accepted that the only sources capable of supplying the energy required to accelerate the bulk of Galactic cosmic rays are supernova explosions, and even though the mechanism of particle acceleration in expanding supernova remnant (SNR) shocks is thought to be well understood, unequivocal evidence for the production of high-energy particles in supernova shells has proven remarkably hard to find. Here we report on observations of the Galactic shell-type SNR RX J1713.7-3946 (G347.3-0.5), which was discovered by ROSAT¹ in X-rays and later claimed as a source of high-energy gamma rays^{2,3} of TeV energies (1 TeV = 10¹² eV). We present a TeV gamma-ray image of the SNR, resolved on arc minute scales, which clearly

shows a shell morphology similar to that seen in X-rays (Fig. 1), thus providing the first direct proof that very-high-energy particles are accelerated in SNR shells. The characteristics of the energy spectrum imply efficient acceleration of charged particles to energies beyond 100 TeV, consistent with current ideas of particle acceleration in young SNR shocks.

RX J1713.7-3946, together with several other southern hemisphere SNRs, is a prime target for observations with the High Energy Stereoscopic System (H.E.S.S.), a new system of four imaging atmospheric Cherenkov telescopes located in the Khomas Highland of Namibia. H.E.S.S.^{4,5} (the name is also a tribute to V. F. Hess, the discoverer of cosmic rays) exploits the most effective detection technique for very-high-energy gamma rays, the stereoscopic imaging of Cherenkov light from air showers. The imaging atmospheric Cherenkov technique, which was pioneered by the Whipple collaboration⁶, makes use of the fact that whenever a high-energy gamma ray hits the Earth's atmosphere, it is absorbed and initiates a cascade of interactions with air atoms leading to the formation of a shower of secondary charged particles. Those travelling faster than the local speed of light in air emit Cherenkov radiation which results in a brief flash of blue Cherenkov light detectable at ground level. By using a telescope with sufficient mirror area to collect enough of the faint light signal, and a fast camera with fine pixelation, one can image the shower and reconstruct from this image the direction and energy of the primary gamma ray. Combined with the approach of stereoscopic imaging of the cascade using a system of telescopes, as pioneered by the HEGRA collaboration⁷, this yields a very powerful technique⁷ for imaging and obtaining energy spectra of astronomical sources at TeV energies. The H.E.S.S. experiment consists of four 13 m diameter telescopes⁸ spaced at the corners of a square of side 120 m, each equipped with a 960 phototube camera⁹ covering a large field of view of diameter 5 degrees. Construction of the telescope system started in 2001; the full array was completed in December 2003 with the commissioning of the fourth telescope. H.E.S.S. has an angular resolution of a few arc minutes, an effective energy range from 100 GeV to 10 TeV with energy resolution of 15 to 20 per cent and a flux sensitivity approaching 10^{-13} erg cm⁻² s⁻¹. These characteristics, together with its southern

hemisphere location, make H.E.S.S. ideally suited for spectroscopic and morphological studies of Galactic Plane sources such as RX J1713.7-3946, which is now the first SNR shell to be confirmed as a TeV source. TeV emission has also been reported from the remnant of SN 1006¹⁰, a result which could so far not be confirmed by H.E.S.S.¹¹, and from Cassiopeia A^{12,13} (a classical core-collapse SNR and the weakest TeV source yet reported) whose northern location makes it inaccessible to H.E.S.S.

In this paper we present results from observations of RX J1713.7-3946 performed between May and August 2003 during two phases of the construction and commissioning of H.E.S.S.. In the first phase, two telescopes were operated independently with stereoscopic event selection done offline using GPS time stamps to identify coincident events. During the second phase, also using two telescopes, coincident events were selected in hardware using an array level trigger. The total on-source observation time was 26 hours; after run selection and dead time correction a dataset corresponding to 18.1 live hours was used in this analysis. At the trigger level (for the observation altitude angles of 60 to 75 degrees), the energy thresholds for the two configurations were 250 GeV (without the array level trigger) and 150 GeV (with the array level trigger). In this analysis hard cuts were used to select only well reconstructed showers. This primarily served to drastically reduce the number of background cosmic-ray events, but it also homogenised these data taken with the two different configurations and improved the angular resolution. Thereby systematic errors are greatly reduced at the expense of a higher energy threshold (\approx 800 GeV for the combined dataset).

Fig. 2 shows the resulting count map centred on RX J1713.7-3946. The SNR stands out from the residual charged cosmic-ray background with a significance of 20 standard deviations. The overall shell structure is clearly visible and coincides closely with that seen in X-rays (see Fig. 1). This is the first case where the identification of an active, i.e. accelerating, celestial gamma-ray source (as opposed to a passive cloud or density enhancement, merely penetrated by energetic particles which are accelerated elsewhere) can be based, not just on a positional coincidence, but on

the image morphology. The overall flux above 1 TeV is $(1.46 \pm 0.17 \text{ (statistical)} \pm 0.37 \text{ (systematic)}) \times 10^{-7}$ photons $\text{m}^{-2}\text{s}^{-1}$ which corresponds to 66 per cent of the Crab Nebula flux as measured by H.E.S.S.. More elaborate analyses of these data using different background models (needed to determine the spectrum) and independent (and different) analysis chains confirm the results presented here.

The energy spectrum of the whole remnant is shown in Fig. 3. These data are well described by a power law (see caption of Fig. 3) with a photon index $\Gamma = 2.19 \pm 0.09 \pm 0.15$, as compared to the photon index of $2.84 \pm 0.15 \pm 0.20$ reported by the CANGAROO collaboration for the northwest part of the SNR³. The integral energy flux between 1 TeV and 10 TeV is estimated to be 3.5×10^{-11} erg $\text{cm}^{-2} \text{s}^{-1}$ which is an order of magnitude smaller than the non-thermal X-ray flux. More data will be taken with the full H.E.S.S. array in 2004. The increased sensitivity (four instead of two telescopes) will enable spatially resolved spectral studies which will be reported in the near future.

RX J1713.7-3946 (situated in the Galactic plane, in the constellation Scorpius) is one of the brighter Galactic X-ray SNR¹⁴ with a flux density of a few times 10^{-10} erg $\text{cm}^{-2} \text{s}^{-1}$. In X-rays it exhibits typical shell morphology, but remarkably the X-ray spectrum is completely dominated by a non-thermal continuum with no detectable line emission. The most plausible origin of these X-rays is the synchrotron radiation of 100 TeV electrons^{15,16}. However, since alternative explanations are not absolutely ruled out¹⁷, only the detection of TeV emission from this SNR provides unambiguous evidence for acceleration of particles to multi-TeV energies. Another important point is that the TeV signal may contain a component due to accelerated protons interacting with the ambient gas as has been predicted theoretically^{18,19}. The contribution of this component should be significantly enhanced when the supernova shell overtakes nearby dense molecular clouds²⁰, as seems to be the case for this object. The CO data²¹ suggest a cloud is interacting with the northwest part of the SNR where a striking spatial coincidence between the CO density peaks and the regions of peak X-ray

emission is seen. The X-ray data²² also indicate significant absorption column densities in the western part of the remnant, at values about twice those to the east. These indications fit qualitatively with the gamma-ray image presented here, where TeV emission is seen from the whole SNR shell but with an increased flux from the northwest side.

Given the recent estimates^{21,22,23} of the distance to the source of 1 kpc, were a significant part of the TeV flux to be formed by interactions of cosmic ray nuclei with gas atoms in the cloud with density n exceeding 100 cm^{-3} , the energetics implied by the gamma-ray flux and the spectrum would be a few times $10^{49} n^{-1} \text{ erg}$ between 10 and 100 TeV. This is consistent with the picture of an SNR origin of Galactic cosmic rays involving about 10 per cent efficiency for conversion of the mechanical energy of the explosion into non-thermal particles, and a production spectrum in the SNR which is approximately an E^{-2} power-law from several GeV to about a PeV. Moreover the gamma-ray morphology is qualitatively what one would expect from particles accelerated at the shock interacting and radiating in the compressed post-shock region. The extension of the gamma-ray spectrum up to energies of 10 TeV (see Fig. 3) requires an extremely effective accelerator boosting particles up to energies of at least 100 TeV. RX J1713.7-3946 is a complex object interacting with molecular clouds of different densities where the TeV emission might emerge from various processes. Without doubt there will be a contribution from energetic electrons through the Inverse Compton process, especially from low density regions (as in the east part) of the SNR. At the elevated densities likely to exist in the northwest rim, π^0 -decays following proton-proton interactions, but also non-thermal Bremsstrahlung of electrons could make a significant contribution. Although disentangling the relative contributions of the various processes is difficult, it should be possible through spatially resolved multi-wavelength studies which will be undertaken with the full H.E.S.S. array. In summary, the first multi-TeV image of a shell-type supernova remnant presented here constitutes a significant step forward towards a solution of the longstanding puzzle of the origin of Galactic cosmic rays as well as marking the birth of a new astronomical

imaging technique operating at photon energies some twelve decades higher than those of visible light.

1. Pfeffermann, E. & Aschenbach, B., in *Röntgenstrahlung from the Universe*. (eds Zimmermann, H. U., Truemper, J. E. & Yorke, H.) (MPE Report 263, Garching, 1996).
2. Muraishi, H. et al. Evidence for TeV gamma-ray emission from the shell type SNR RX J1713.7-3946. *Astron. Astrophys.* **354**, L57-L61 (2000).
3. Enomoto, R. et al. The acceleration of cosmic-ray protons in the supernova remnant RX J1713.7-3946. *Nature* **416**, 823-826 (2002).
4. Hinton, J. A. (H.E.S.S. Collaboration) The status of the HESS project. *New Astronomy Reviews* **48**, 331-337 (2004).
5. Hofmann, W. (H.E.S.S. Collaboration) Status of the H.E.S.S. project. *Proc. 28th ICRC*, Tsukuba, Univ. Academy Press, Tokyo, 2811-2814 (2003).
6. Weekes, T. C. et al. Observation of TeV gamma rays from the Crab nebula using the atmospheric Cherenkov imaging technique. *Astrophys. J.* **342**, 379-395 (1989).
7. Aharonian, F. A. et al. The time averaged TeV energy spectrum of Mkn 501 of the extraordinary 1997 outburst as measured with the stereoscopic Cherenkov telescope system of HEGRA. *Astron. Astrophys.* **349**, 11-28 (1999).
8. Bernlöhr, K. et al. The optical system of the H.E.S.S. imaging atmospheric Cherenkov telescopes, Part I: layout and components of the system. *Astropart. Phys.* **20**, 111-128 (2003).
9. Vincent, P. et al. Performance of the H.E.S.S. cameras. *Proc. 28th ICRC*, Tsukuba, Univ. Academy Press, Tokyo, 2887-2990 (2003).

10. Tanimori, T. et al. Discovery of TeV Gamma Rays from SN 1006: Further Evidence for the Supernova Remnant Origin of Cosmic Rays. *Astrophys. J.* **497**, L25-L28 (1998).
11. Masterson, C. (H.E.S.S. Collaboration) Observation Of Galactic TeV Gamma Ray Sources With H.E.S.S.. *Proc. 28th ICRC*, Tsukuba, Univ. Academy Press, Tokyo, 2323 - 2326 (2003).
12. Aharonian, F. A. et al. Evidence for TeV gamma ray emission from Cassiopeia A. *Astron. Astrophys.* **370**, 112-120 (2001).
13. Berezhko, E. G., Pühlhofer, G., Völk, H. J. Gamma-ray emission from Cassiopeia A produced by accelerated cosmic rays. *Astron. Astrophys.* **400**, 971-980 (2003).
14. Slane, P. et al. Nonthermal X-ray emission from the shell-type supernova remnant G347.3-0.5. *Astrophys. J.* **525**, 357-367 (1999).
15. Ellison, D. C., Slane, P., Gaensler, P. M. Broadband Observations and Modeling of the Shell-Type Supernova Remnant G347.3-0.5. *Astrophys. J.* **563**, 191-201 (2001).
16. Uchiyama, Y., Aharonian, F. A., Takahashi, T. Fine-structure in the nonthermal X-ray emission of SNR RX J1713.7-3946 revealed by Chandra. *Astron. Astrophys.* **400**, 567-574 (2003).
17. Laming, J. M. A Thermal Model for the Featureless X-Ray Emission from SN 1006? *Astrophys. J.* **499**, 309-314 (1998).
18. Drury, L. O'C, Aharonian, F. A., Völk, H. J. The gamma-ray visibility of supernova remnants. A test of cosmic-ray origin. *Astron. Astrophys.* **287**, 959-971 (1994).
19. Naito, T. & Takahara, F. High-energy gamma-ray emission from supernova remnants. *J. Phys. G* **20**, 477-486 (1994).
20. Aharonian, F. A., Drury, L. O'C, Völk, H. J. GeV/TeV gamma-ray emission from dense molecular clouds overtaken by supernova shells. *Astron. Astrophys.* **285**, 645-647 (1994).
21. Fukui, Y. et al. Discovery of Interacting Molecular Gas toward the TeV Gamma-Ray Peak of the SNR G 347.3-0.5. *Publ. Astron. Soc. Japan* **55**, L61-L64 (2003).

22. Cassam-Chenaï, A. et al. XMM-Newton observations of the supernova remnant RX J1713.7-3946 and its central source. *Astron. Astrophys.* **in press** (2004).
23. Koo, B., Kang, J., McClure-Griffiths, N. HI Study of Southern Galactic Supernova Remnants. IAU Symposium *Young Neutron Stars and Their Environments* (eds. Camilo, F. & Gaensler, B.M.), Vol. **218**, 85 (2004).
24. Uchiyama, Y., Takahashi, T., Aharonian, F. A. Flat Spectrum X-ray Emission from the Direction of a Molecular Cloud Associated with SNR RX J1713.7-3946. *Publ. Astron. Soc. Japan* **54**, L73 (2002).

Acknowledgements The support of the Namibian authorities and of the University of Namibia in facilitating the construction and operation of H.E.S.S. is gratefully acknowledged, as is the support by the German Ministry for Education and Research (BMBF), the Max Planck Society, the French Ministry for Research, the CNRS-IN2P3 and the Astroparticle Interdisciplinary Programme of the CNRS, the U.K. Particle Physics and Astronomy Research Council (PPARC), the IPNP of the Charles University, the South African Department of Science and Technology and National Research Foundation, and by the University of Namibia. We appreciate the excellent work of the technical support staff in Berlin, Durham, Hamburg, Heidelberg, Palaiseau, Paris, Saclay, and in Namibia in the construction and operation of the equipment. The authors also thank Y. Uchiyama for kindly supplying the ASCA X-ray data shown in Fig. 1.

Competing interests statement The authors declare that they have no competing financial interests.

Correspondence should be addressed to David.Berge@mpi-hd.mpg.de

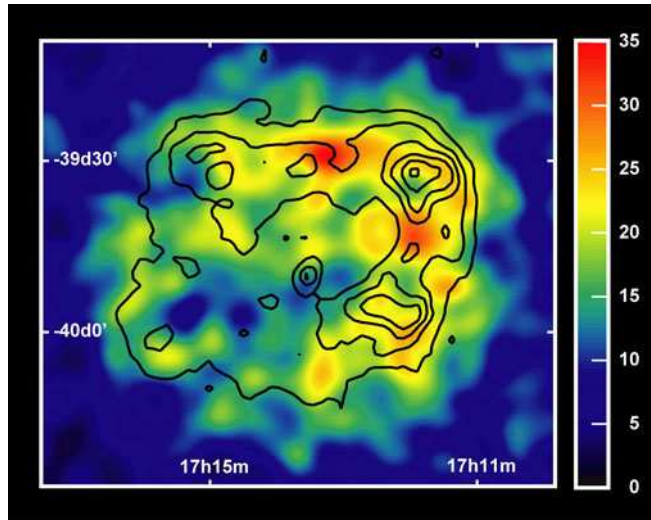


Figure 1 Gamma-ray image of the SNR RX J1713.7-3946 obtained with the H.E.S.S. telescopes. It represents the first ever astronomical image in the TeV energy regime. Hard cuts were applied to select well-reconstructed gamma-like events above 800 GeV. The image is smoothed with a Gaussian of standard deviation 3 arc minutes (matched to the angular resolution of the instrument for this particular dataset). The linear colour scale is in units of counts. It is important to note that no background subtraction or camera-efficiency corrections have been applied. This demonstrates that the structures seen are not artefacts of the analysis but real and visible in the raw post-cuts data (the background in the field of view is at a level of about five counts and the efficiency across the SNR changes by less than ten per cent). This image, obtained with a partial array during construction, impressively demonstrates the ability of H.E.S.S. to map extended objects. The superimposed (linearly spaced) contours show the X-ray surface brightness as seen by ASCA in the 1-3 keV range for comparison²⁴. Note that the angular resolution of ASCA is comparable to that of H.E.S.S. which enables direct comparison of the two images.

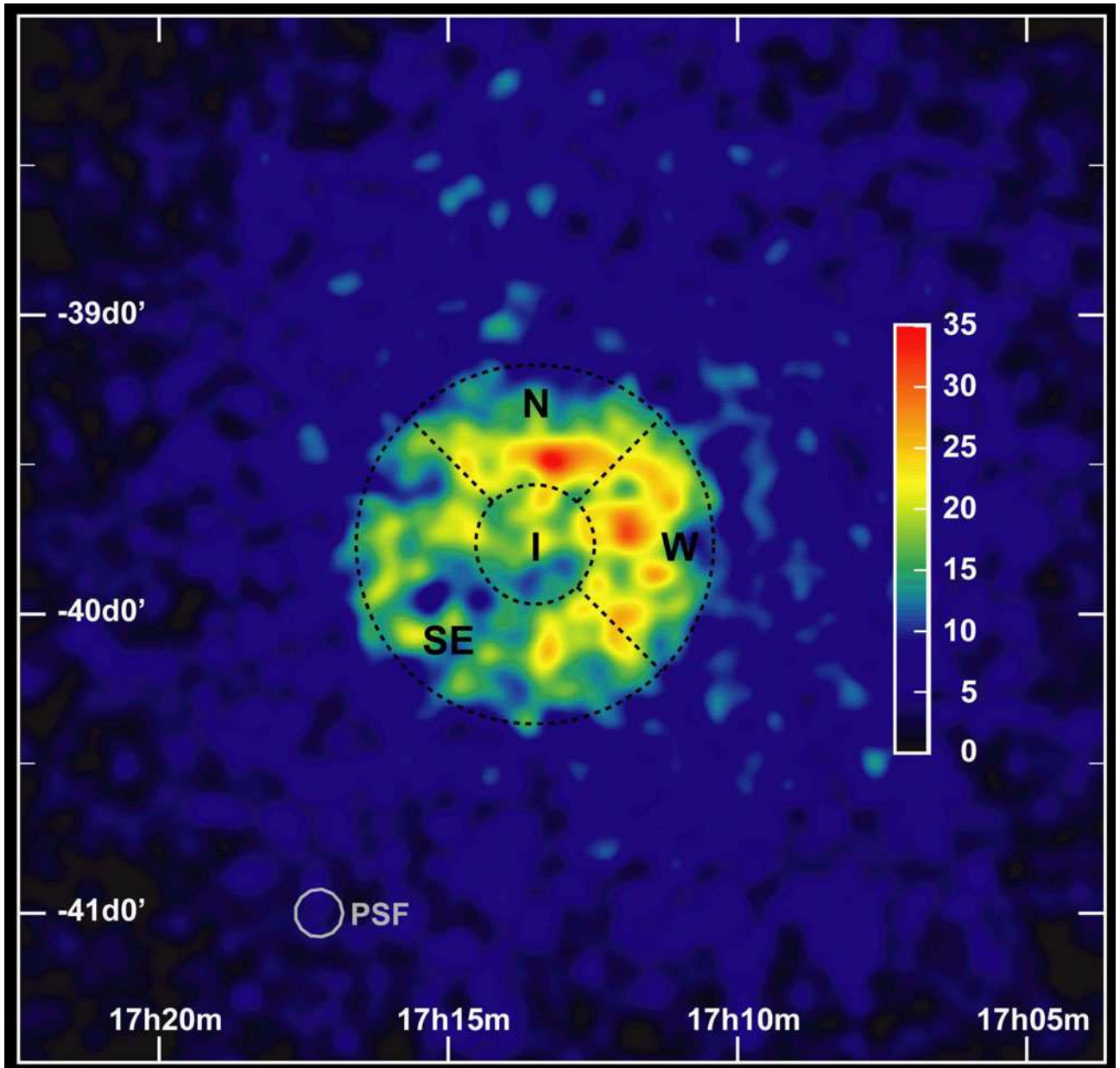


Figure 2 Wide field of view (3.5 by 3.5 degrees) around RX J1713.7-3946. Integration regions for flux estimates are shown. The flux above 1 TeV from the northern (N) rim is $(3.0 \pm 0.6) \times 10^{-8}$ photons $\text{m}^{-2} \text{s}^{-1}$, from the west (W) rim $(4.1 \pm 0.8) \times 10^{-8}$ photons $\text{m}^{-2} \text{s}^{-1}$, from the southeast (SE) rim $(5.9 \pm 1.0) \times 10^{-8}$ photons $\text{m}^{-2} \text{s}^{-1}$ and the flux from the interior (I) $(1.7 \pm 0.6) \times 10^{-8}$ photons $\text{m}^{-2} \text{s}^{-1}$. The mean gamma-ray brightnesses per unit solid angle (i.e. the flux values normalised to the area) of the regions are in the ratio 1 : 1.4 : 1 : 1.2 (N : W : SE : I). These values might contradict the visual impression that the northwest shell of the SNR is brighter. However, statistics of the data sample are limited and the different areas were chosen for geometric reasons. Looking at the image one sees for

example that dim regions are included in the seemingly brighter northern and western area whereas the interior might gain from leakages from the northwest shell. More detailed spatially resolved flux-studies will have to await the advent of new data taken with the full H.E.S.S. array with increased sensitivity. The 70% containment radius of the gamma-ray point-spread-function (PSF) for this dataset with an energy threshold of 800 GeV is illustrated in the bottom left hand corner (structures which are smaller than this circle should not be considered as real). The map is smoothed as in Fig. 1, having the same scale in units of counts. Note that the efficiency of the camera falls off towards the edge of the field of view.

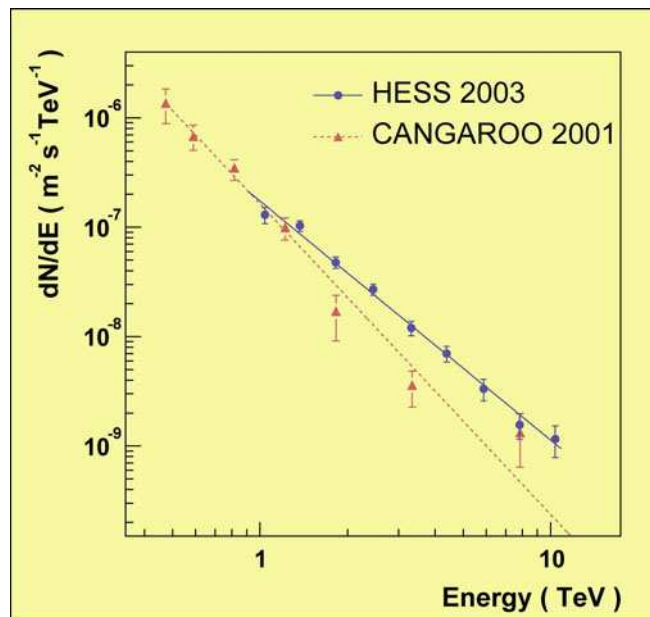


Figure 3 Gamma-ray energy spectrum of RX J1713.7-3946 as measured with the H.E.S.S. telescopes. These data (blue solid circles) can be described by a power law: $dN/dE \propto E^{-\Gamma}$, the best fit result (blue solid line) gives $\Gamma = 2.19 \pm 0.09$ (statistical) ± 0.15 (systematic) with $\chi^2 = 5.9$ with 7 degrees of freedom. The integral flux above 1 TeV is found to be $(1.46 \pm 0.17$ (statistical) ± 0.37 (systematic)) $\times 10^{-7}$ photons $m^{-2}s^{-1}$. There is clearly no evidence for a cut-off in the data, but if one nevertheless attempts to fit an exponentially cut-off power-law of the form $dN/dE \propto E^{-\Gamma_c} e^{-E/E_c}$, the minimum acceptable value of E_c is 4 TeV with a very hard photon index of $\Gamma_c = 1.5$. The spectral data points

reported by the CANGAROO collaboration³ for the northwest part of the remnant are shown for comparison as red triangles, the best fit result as a dashed red line. The fact that CANGAROO reported a spectrum only for a part of the SNR prohibits at this stage a definite statement about the compatibility of the two measurements. Error bars always give the 1σ statistical errors.